Ionization and dissociation of H_2 in a static electric field: Levels near the ionization threshold

Wallace L. Glab* and Jan P. Hessler

Chemistry Division, Argonne National Laboratory, 9700 South Cass Avenue, Argonne, Illinois 60439

We have made high-resolution measurements of the photoionization and photodissociation spectra of molecular hydrogen in the energy region near the first ionization limit in a strong, static, external electric field. We find that below the classical field-ionization energy $E_c = -2\sqrt{F}$ electric-field-induced predissociation is a dominant decay mechanism for many of the highly excited Stark components, while above the classical field-ionization energy there is a competition between field-induced ionization and dissociation. We have also observed forced autoionization of the $(1s\sigma 7p\sigma)^1\Sigma_u^+(v=1, J=1$ and 2) levels through their coupling with the structured continuum of highly excited Stark states, leading to enhanced ionization and dissociation through those Stark states that are nearly degenerate with them.

I. INTRODUCTION

Over the last decade, a number of studies have been made of the effects of an external, static, electric field on highly excited Rydberg levels of atomic systems. In particular, the regime where the forces due to the external field and the attractive field of the ionic core are nearly comparable has received a great deal of interest. Theoretical approaches were developed first for atomic hydrogen, for which the problem was solved with numerical techniques,[1] and later for complex atoms using multichannel quantum defect theory.[2] Experimentally, complex atoms were studied first[3] due to the relative ease by which their high-lying levels can be excited. More recently, advances in multiphoton excitation techniques and nonlinear techniques to generate tunable vacuum-ultraviolet light have made thorough studies of the strong-field Stark effect in atomic hydrogen possible.[4] The observed features of the photoionization spectra of atomic systems in electric fields are now well understood for both simple and complex atoms.[5]

In contrast to the situation for atoms, the effects of a strong external field on the highly excited Rydberg levels of simple, diatomic molecules such as H_2, Na_2, and Li_2 are just beginning to be investigated. For example, Stark splitting[6] and electric-field-hindered autoionization[7] have been observed in the $nd\,^1\Lambda_g$ Rydberg series of Na_2, electronic-field-induced ionization and forced autoionization[8] have been observed in Li_2, and studies of the field-ionization threshold[9] in H_2 have confirmed the $1/16n_s^4$ behavior seen in atomic systems. Unfortunately, none of these studies has addressed a fundamental difference between the atomic and molecular cases, i.e., the presence in the molecular case of the dissociative decay channel.

In this paper, we report results of an experimental study of the ionization and dissociation spectra of high-lying, singlet, np, Rydberg levels of H_2 in an external electric field. The energy region from just below the classical field-ionization energy $E_c = -2\sqrt{F}$ (atomic units) to

the zero-field adiabatic ionization potential is emphasized. We only consider levels with energies below the zero-field ionization potential of the molecule. High-lying Stark states of H_2 are excited using the two-step, two-photon resonant, three-photon excitation scheme we used previously to study field-free high np Rydberg levels.[10] Briefly, Doppler-free spectra are obtained by exciting the two-photon transition between the ground and $[1s\sigma 2s\sigma + (2p\sigma)^2]^1\Sigma_g^+$ electronic surfaces with a single narrow-band light beam. After a delay of a few nanoseconds, another pulse of light is used to excite the high-Rydberg levels. We observe sharp resonant structure in photoionization near and above the classical field-ionization energy. Many states which lie below the classical field-ionization energy undergo electric-field-induced predissociation. The rates for ionization and dissociation are comparable for Stark states just above the classical field-ionization energy. Moreover, we find that the relative importance of the two decay channels depends on the orientation of the state's charge distribution relative to the field direction as well as the level of mixing induced by the electric field. Also, above the classical field-ionization energy and below the zero-field ionization threshold, we observe forced autoionization of the $(1s\sigma 7p\sigma)^1\Sigma_u^+(v=1, J=1$ and 2) levels through the interaction of these levels with the highly-excited Stark states.

Because the dynamic properties of the Rydberg levels of H_2 are crucial to our discussion, we briefly review, in Sec. II, the spectroscopic and dissociative properties of the high, np, Rydberg levels in the absence of an electric field. This section also reviews the theoretical framework within which the Stark effect of atomic systems is treated, describes the new effects which may be expected to arise in molecular systems, and establishes the notation used in subsequent sections. We describe the experimental approach in Sec. III. We present the results of low- and high-resolution studies of the ionization and dissociation spectra of H_2 in an electric field in Sec. IV, and discuss

them in terms of the theory presented in Sec. II. Conclusions and suggestions for future work are presented in Sec. V.

II. PROPERTIES OF THE RYDBERG LEVELS OF H_2 AND STARK STATES NEAR AND ABOVE THE CLASSICAL FIELD-IONIZATION ENERGY

A. General comments on molecular Rydberg levels

The differences between atoms and molecules in high-Rydberg levels result from the vibrational and rotational structure of the molecular-ion core and the dissociative decay channel. The molecular structure of the ionic core complicates the interpretation of absorption measurements just below the first ionization potential since a Rydberg series converges to every vibrational-rotational level of the ionic core. For sufficiently high principle quantum number, this means that the electronic levels are more closely spaced than vibrational and even rotational levels of the core. Conversely, the behavior of an electron in a high-Rydberg level of a molecule is similar to atomic systems since each consists of a core ion and an electron at a large mean distance from the core. For sufficiently high principle quantum numbers $n \geq 10$ the molecular core can be approximated by a non-Coulombic charge distribution, so a complex atom, such as calcium, strontium, or barium, is a useful prototype for the Rydberg levels of molecular hydrogen. Within this context, the energy levels for a Rydberg series converging on the vibrational-rotational levels of the ion denoted by v^+ and N^+ follow the modified Rydberg formula

$$E(n, v^+, N^+) = [V_{ion} + E_{ion}(v^+, N^+)] - \frac{\mathscr{R}}{(n - \delta_l)^2} . \quad (1)$$

The adiabatic ionization potential of the molecule is V_{ion}, the energy of the level of the ion with respect to the adiabatic ionization potential to which the series is converging is $E_{ion}(v^+, N^+)$, the principle quantum number is n, the quantum defect is δ_l which depends upon the orbital angular momentum l of the electron, and $\mathscr{R}$ is the Rydberg constant for H_2, $109\,707.42$ cm^{-1}. The mean value of the orbital radius $\langle r_{nl} \rangle$ is given by

$$\langle r_{nl} \rangle = \frac{a_0}{2Z}[3n^2 - l(l+1)] , \quad (2)$$

where the Bohr radius is a_0 and Z is the number of electronic charges for the molecular-ion core. For an electron with $n = 30$ and little orbital angular momentum $\langle r \rangle = 70$ nm which is approximately 700 times greater than the internuclear separation in the molecular-ion core.

B. Spectroscopy and dissociative dynamics of H_2 Rydberg levels

Because of the complex nature of the Rydberg spectra of molecular systems, measurements of the high-Rydberg series in H_2 were not published until 1969, at which time both Herzberg[11] and Takezawa[12] presented results within a short time of one another. The np Rydberg series was

first analyzed in terms of a two-channel quantum-defect theory (QDT) by Herzberg and Jungen.[13] Later, the multichannel quantum-defect theory (MQDT) was used to compute the positions of the low-lying levels[14] and then extended to include rotational and vibrational preionization and predissociation.[15] Recently, the application of MQDT to molecular systems has been reviewed.[16] Briefly, the Rydberg spectra of H_2 involve excitation from levels within the $(1s\sigma)^2\,{}^1\Sigma_g^+$ ground electronic potential surface to the np-Rydberg levels. The Rydberg series accessible from the ground electronic surface consist of two interacting series of even symmetry $(1s\sigma np\sigma)\,{}^1\Sigma_u^+$ and $(1s\sigma np\pi)\,{}^1\Pi_u^+$ and a third noninteracting series of odd symmetry $(1s\sigma np\pi)\,{}^1\Pi_u^-$. The odd and even symmetry designations refer to the reflection symmetry of the electronic wave function with respect to reflection about any plane containing both nuclei.[17] The levels of the various series are not degenerate. This is due to the breakdown of the Born-Oppenheimer approximation which leads to electronic-rotational coupling. The quantum defect[10] for the pure $np\pi$ members is -0.082 and for the pure $np\sigma$ members $+0.196$. Therefore, deviations from the complex-atom approximation, in which the quantum defect depends only on the orbital angular momentum of the electron, are slight. Indeed, calculations indicate that the quantum defects of the d, f, etc. Rydberg series of H_2 are all rather small.[18] We will now examine, in some detail, the dissociative properties of the Rydberg states of H_2.

The dissociative properties of the lower members of the np-Rydberg series $n = 3$ to 9 have been studied by comparing excitation spectra of Lyman-α fluorescence[19-22] with absorption spectra.[23] Specifically, even-symmetry levels from the $(1s\sigma 3p\pi)\,{}^1\Pi_u$ potential curve have the highest dissociative rates[24] $\approx 10^{12}$ s^{-1}. Of these, the low vibrational levels are rotationally coupled[25,26] to the $(1s\sigma 3p\sigma)\,{}^1\Sigma_u^+$ continuum and the higher vibrational levels are coupled to predissociative levels from the $(1s\sigma 4p\sigma)\,{}^1\Sigma_u^+$ potential curves. For convenience, we show in Fig. 1 the singlet potential-energy curves[27] for H_2. The dissociative rates for odd-symmetry levels from the $(1s\sigma np\pi)\,{}^1\Pi_u$ potential curves $n = 4$ to 9 are several orders of magnitude slower[28] than the rates of the even-symmetry level from the $(1s\sigma 3p\pi)\,{}^1\Pi_u$ surface. These dissociations are not due to direct coupling to a dissociative continuum. Therefore, the dissociative rates vary irregularly with the vibrational quantum number; this is characteristic of accidental predissociation.[29] Specifically, even symmetry levels within the $(1s\sigma np\pi)\,{}^1\Pi_u$ potential curves can couple to the $(1s\sigma 3p\sigma)\,{}^1\Sigma_u^+$ dissociative continuum via two interfering paths: (a) the levels from $(1s\sigma np\pi)\,{}^1\Pi_u^+$ curve are strongly coupled by rotation with levels from the $(1s\sigma np\sigma)\,{}^1\Sigma_u^+$ curve which predissociate by the strong vibrational coupling to the $(1s\sigma 3p\sigma)\,{}^1\Sigma_u^+$ continuum and (b) a vibrational coupling can weakly mix levels from the $(1s\sigma np\pi)\,{}^1\Pi_u^+$ curve with those of the $(1s\sigma 3p\pi)\,{}^1\Pi_u^+$ curve which are strongly predissociated through a rotational coupling to the $(1s\sigma 3p\sigma)\,{}^1\Sigma_u^+$ dissociative countiuum. For our discussion, it is sufficient to note that levels with odd reflection
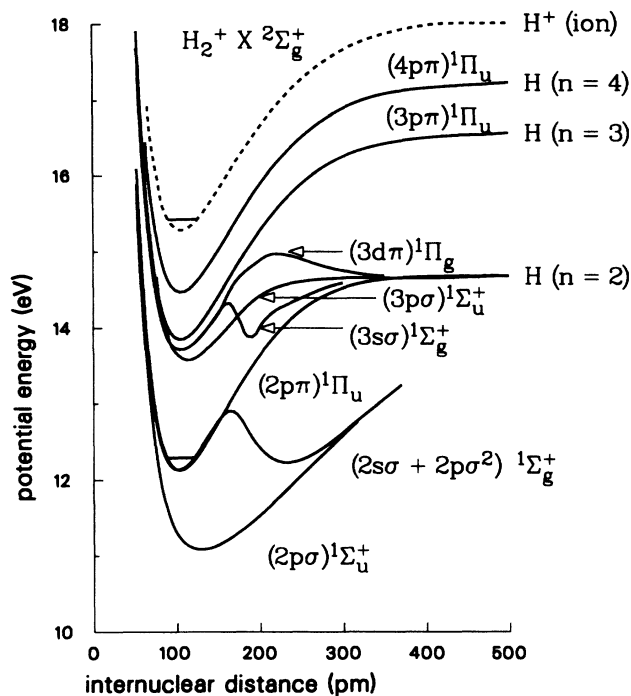
FIG. 1. Singlet potential-energy curves for H_2. To save space $1s\sigma$ has been omitted from electronic configuration designations. The excited dissociative product is shown on the right-hand side. For example, $H(n=2)$ means the molecule will dissociate into a hydrogen atom in the $2s$ or $2p$ configuration plus a hydrogen atom in the $1s$ configuration.

symmetry are forbidden to interact with the dissociative continuum of the $(1s\sigma 3p\sigma)^1\Sigma_u^+$ configuration. Therefore, they are stable with respect to dissociation, except possibly very weakly through a vibronic or dynamic interaction with the continuum of the $(1s\sigma 2p\pi)^1\Pi_u^-$ potential curve. On the other hand, levels of even symmetry can couple accidently to the dissociative continuum. It is the symmetry property of the electronic wave function which determines if the dissociative channel is open and, of course, the detailed make up of the wave function which determines the dissociative rate. The powerful role of symmetry has been beautifully illustrated by fluorescent lifetime measurements[30] of the $(1s\sigma 3p\pi)^1\Pi_u^-$ levels of H_2. The measured decay rates are approximately equal to 4×10^8 s^{-1} and agree with the calculated radiative transition rates. These results show that the dissociative probability for the odd-symmetry levels is more than 6000 times smaller than the dissociative probabilities observed for the even-symmetry $(1s\sigma 3p\pi)^1\Pi_u^+$ components.

With regard to dissociation of the high-Rydberg levels, we reported[10] Doppler-free measurements of the high-np-Rydberg levels $n\leq90$ and monitored the dissociative decay channel by ionizing the $H(n=2)$ atomic products. We observed significant predissociation in the ortho-H_2 Rydberg levels up to $n\approx50$ with a wide range of predissociative rates. In particular, we found strong predissociation in the region of $n=24$ and 34 which is consistent

with accidental predissociation of the Rydberg levels by the $(1s\sigma 4p\sigma)^1\Sigma_u^+(v=4, J=0)$ and $(1s\sigma 7p\sigma)^1\Sigma_u^+(v=1, J=2)$ levels, which are known to predissociate.[31] We have made more recent measurements at higher resolution[32] which indicate that only even-symmetry levels which correlate to $^1\Sigma_u^+$ or $^1\Pi_u^+(J=0$ and 2) predissociate while odd-symmetry levels which correlate to $^1\Pi_u^-(J=1)$ are stable with respect to dissociation. As with the lower members of the Rydberg series, the symmetry of the electronic wave function determines whether the dissociative decay channel is open. We note, since the radiative decay rates of high-Rydberg levels are very slow, $\approx10^9/n^3$ s^{-1}, even rather low dissociative rates can dominate the dynamical behavior of molecular systems in high-Rydberg levels.

C. Stark effect on Rydberg levels

The Stark effect on a system with a Coulombic core potential (i.e., atomic hydrogen) is most easily discussed by solving the nonrelativistic Schrödinger equation in parabolic coordinates[33] (ξ, η, and ϕ). This permits the wave functions to be described by

$$\psi(\xi,\eta,m)=U_1(\xi)U_2(\eta)e^{\pm im\phi} \quad (m\geq0) , \tag{3}$$

which leads to two identical equations for the functions U_1 and U_2 for the case of zero field. These can be expressed in terms of Laguerre polynomials. In parabolic coordinates, the eigenvalues are the separation parameters Z_1 and Z_2 and the eigenfunctions are characterized by the parabolic quantum numbers n_1 and n_2 and the orbital magnetic quantum number m. The principle quantum number n defined from the solution in spherical coordinates is related to the parabolic quantum numbers by the equation

$$n=n_1+n_2+|m|+1 . \tag{4}$$

The parabolic quantum numbers are positive integers or zero and are related to the separation parameters by the expression

$$Z_1-Z_2=(n_1-n_2)/n . \tag{5}$$

To obtain the energy of the system the relationship

$$Z=Z_1+Z_2 \tag{6}$$

is used where Z is the total charge of the core. The magnetic quantum number m is restricted by $0\leq m\leq n-1$. Note, in parabolic coordinates the orbital angular momentum of the electron is no longer associated with a single eigenfunction.

To include the effect of an electric field in the z direction, the Stark term $\frac{1}{2}F(\xi-\eta)$ is added to the Hamiltonian. The separation of variables described by Eq. (3) still holds, but the differential equations for U_1 and U_2 differ by the sign of the electric-field-dependent term. From first-order perturbation theory there is no mixing between levels with different principle quantum numbers and the energy of a state is given by

$$E=-\frac{Z^2}{2n^2}+\frac{3Fn}{2Z}(n_1-n_2) . \tag{7}$$

The difference in the quantum numbers $n_1 - n_2$ is called the "electric quantum number." The Stark states have charge distributions which are asymmetric with respect to the $z = 0$ plane. States with positive $n_1 - n_2 (Z_1 \approx 1)$ are extended in the upfield direction where the Coulomb potential and the electric potential combine to give a raised potential barrier; thus, their energies are shifted to the blue. Conversely, states with negative values of $n_1 - n_2 (Z_1 \approx 0)$ extend to the downfield direction where they sample more of the lowered potential barrier and are consequently red shifted.

The terms of the perturbation expansion for the energies of hydrogenic Stark states have been calculated to arbitrary order.[34] However, the perturbation expansion is known to be divergent,[35] and gives inaccurate results for states with energies well above the top of the lowered barrier of the combined potential, known as the saddle-point energy. This is to be expected, since the field's effect on the electron motion is strong in this energy region. Below the saddle-point energy fourth-order perturbation theory gives a good approximation to the Stark state energies. For states of higher energy, non-perturbative techniques must be used since the field is no longer weak compared to the Coulomb field; in the past, both Wentzel-Kramers-Brillouin[2] and numerical approaches[1,36] have been successfully applied to the hydrogenic Stark problem.

In an electric field, the effective potential in the ξ coordinate produces bound wave functions, whereas the effective potential in the η coordinate produces continuum wave functions. Therefore, all states in an electric field possess a nonvanishing ionization rate. A state's ionization rate depends on its energy relative to the top of the potential barrier and the orientation of its charge distribution relative to the field, i.e., on its parabolic quantum numbers. Classically, the top of the barrier, or saddle point, occurs when the electric force due to the ionic core is just balanced by the external field. At this point, the electric field lowers the potential energy by the amount $E_c = -2\sqrt{F}$. In the case of a pure Coulomb potential, the energy at the top of the barrier depends on the quantum numbers of the state through the value of the separation parameter Z_2, so that $E_c = -2\sqrt{FZ_2}$. This dependence on the value of the separation parameter (and thus on the state's parabolic quantum numbers) reflects the fact that red shifted states ionize more rapidly than blue shifted states of the same energy, since their charge distribution is extended in the direction of the saddle point. A state whose energy lies below this barrier must ionize by tunneling through the barrier, and therefore will have a relatively low rate of ionization.

In a complex system, above the saddle-point energy the non-Coulombic potential of the ionic core causes coupling between stable and ionizing states with the same value of the magnetic quantum number, thereby mixing the states.[37] The ionization rates of most of the states of complex atoms with energies above E_c are due primarily to their core-induced coupling to the ionization continua of "open" parabolic channels, and thus depend sensitively on the quantum defects of the series. Since the ionization is due to the coupling of a quasistable state to an un-

derlying continuum, the ionization resonances (if isolated) appear with shapes described by Fano profiles. For systems whose quantum defects for all series are small (such as Li), the Stark effect behavior is nearly hydrogenic, whereas for systems with large quantum defects the resonances are strongly broadened and shifted from their hydrogenic positions. States with $m = 0$ are generally more affected by core mixing than states with $m = 1$, since the $m = 1$ states have no s-wave contribution. The detailed MQDT theory of the Stark effect of complex atoms was presented by Harmin.[2,38]

The photoabsorption probability for excitation of a quasidiscrete state from a low-lying state depends on the charge density of the excited state in the region of the ionic core, and therefore also depends on the values of its separation parameters. For excited states with $m = 0$, the charge density near the nucleus maximizes[2] for $Z_1 \sim 0$ or 1; that is, for states which are nearly "reddest" or "bluest." For excited states with $m = 1$, the charge density maximizes for $Z_1 \sim Z_2 (n_1 - n_2 \sim 0)$. In the case of atomic hydrogen, the photoabsorption probability for excitation from excited states depends in a complicated way on the charge distribution overlap between the initial parabolic state and the final parabolic state.[39] The only strict selection rule which applies to the excitation of the Stark states is that π-polarized light (electric vector along the static field) results in $\Delta m = 0$ transitions, while σ-polarized light (electric vector perpendicular to the static field) results in $\Delta m = \pm 1$ transitions.

D. The case of molecular hydrogen

When an external electric field is applied to molecular hydrogen we anticipate many similarities to complex atoms and a number of new phenomena in the high Rydberg levels.

First, because of the low values of the quantum defects, the energy level structure should behave very similarly to that of nearly hydrogenic atomic systems such as Li. However, ionization through core-induced mixing of closed and open parabolic channels should be the dominant decay mechanism for states with energies above the classical saddle-point energy $E_c = -2\sqrt{F}$. Conversely, below the classical field for ionization, where the electrons must tunnel through the barrier, the dynamics will be controlled primarily by the relative rates for dissociation and fluorescence.

Secondly, the electric field has the effect of destroying the symmetry of the core potential, thereby inducing mixing between levels of even and odd symmetry. This mixing has been used to explain the increased absorption[40] in the neighborhood of optically allowed transitions to $(1s\sigma np\sigma)\,{}^1\Sigma_u^+$ and $(1s\sigma np\pi)\,{}^1\Pi_u$ levels with $n = 4$ to 7. Electric-field-induced predissociation of excited states of molecular hydrogen has been noted previously for low-lying states.[41] Dissociation of high-np-Rydberg levels of ortho-H_2, induced by a pulsed electric field, has recently been observed by our group.[31] Thus we would expect to observe predissociation of the highly excited Stark states caused by field-induced couplings to the dissociative continua; these couplings could either be direct,

or through an accidental degeneracy between the Stark states and a predissociated level of low principle quantum number. A competition between the decay channels of ionization and dissociation would then be expected. The predissociation rates of the Stark states will depend on their charge densities near the core, and will thus have a relatively weak energy dependence much like that of the oscillator strengths for excitation of the states. The ionization rates, however, would be expected to increase more rapidly with energy since they reflect the long-range behavior of the wave function near the lowered barrier of the combined potential. Thus, we can see that the dynamics of the decay of Stark states of a molecule are far more complcated than those of an atomic system.

Furthermore, the additional degrees of freedom resulting from the rotation and vibration of the ionic core lead to a large density of perturbing states which can couple to the highly excited Stark states. States of low principle quantum number which lie between E_c and the zero-field ionization limit $E=0$ are energetically allowed to autoionize, through their coupling to the structured continuum of Stark states arising from the Rydberg levels converging to $E=0$. This phenomenon is referred to as forced autoionization, since a state which is stable for zero applied field can ionize spontaneously in the presence of a field.

Finally, the presence of core rotation will complicate the understanding of the Stark spectra of H_2, since in general m_l is not a good quantum number and the Stark states will be mixtures of various m_l states. The highly excited states of H_2 are well described by Hund's case d coupling,[17] in which the orbital angular momentum of the excited electron is strongly coupled to the rotational angular momentum of the core, but decoupled from the internuclear axis. In a nonzero electric field, the orbital angular momentum is no longer a conserved quantity; therefore, l is not a good quantum number. However, the projection of the angular momentum remains conserved and m_J is a good quantum number. The selection rule for excitation of the Stark states involves m_J. The ortho- and paramodifications of molecular hydrogen remain unmixed in an electric field, implying that when we excite the molecule from an initial state with $J=0$ (parahydrogen) it will make transitions to states converging to the $N^+=0$ and $N^+=2$ rotational states of the ion core, just as in the field-free case. The oscillator strengths of the transitions to the $N^+=2$ series are very small in the zero-field case, and since the oscillator strength is determined by the properties of the excited-state wave function near the core where the electric field has negligible effect, we would expect the $N^+=2$ Stark states to also be only weakly excitable. As in the field-free case, these states will manifest themselves mainly through their perturbation of the states of the $N^+=0$ series. Thus, in para-hydrogen excited from a $J=0$ initial state, π-polarized light will excite $N^+=0$ states with $m_l=0$ and σ-polarized light will excite $N^+=0$ states with $m_l=1$. The $N^+=2$ states (and the states of orthohydrogen) will be mixtures of different m_l states; therefore, their individual Stark components should be excitable with either polarization of light, while the $N^+=0$ series will retain

the polarization dependence of atomic hydrogen. Because the $N^+=0$ series can be more directly compared to hydrogenic theory, we will concentrate on this series in our high resolution work.

A comprehensive theory of the Stark effect for molecular systems, including both the ionization and dissociation decay channels, does not currently exist. However, it seems that all the necessary theoretical tools are available. Jungen[16] has presented a quantum defect theory that treats open ionization and dissociation channels on an equal basis and gives good agreement with experimental results for autoionizing states of H_2. A very recent study[42] applied density-of-states (DOS) theory to the Stark effect on autoionizing states of Na_2, and a similar treatment of the Stark effect of H_2 has also appeared.[43] Neither of these studies allowed for a dissociative decay channel. A modification of Jungen's theory that treats the long-range behavior of the electron's wave function using parabolic coordinate eigenfunctions as in DOS theory would be a likely candidate for a rigorous theory of the Stark effect in H_2.

III. EXPERIMENT

The multiphoton excitation scheme which we use to excite high-lying, singlet, np, Rydberg levels of H_2 has been described previously.[10] Briefly, molecular hydrogen is excited to a single rovibronic level within the $[1s\sigma 2s\sigma + (2p\sigma)^2]\,^1\Sigma_g^+$ potential-energy surface by the simultaneous absorption of two photons at a wavelength of 202 nm. The nonlinear crystal beta-barium borate is used to generate the third harmonic[44] of the output of a single-frequency, ring, dye laser operating at 605 nm,[45] which has been amplified in a chain of traveling-wave dye amplifiers pumped by the second harmonic of an Nd^{3+}:YAG (where YAG denotes yttrium aluminum garnet) laser with a 10-Hz repetition rate. This technique results in much higher pulse energies at 202 nm (~ 1 mJ/pulse) than are achievable through the use of stimulated Raman shifting of the dye laser output, thereby allowing us to perform experiments under collision-free conditions at much lower sample densities. The spectral bandwidth of the 202-nm light is near the Fourier transform limit (~ 150 MHz), since it is free of the broadening which the high-order anti-Stokes output of a Raman shifter has recently been found to exhibit.[46] The molecules, once they have been excited to the E state, are then further excited to the region of the first ionization limit by a second tunable dye laser operating at about 400 nm (0.03-cm^{-1} bandwidth, 0.5-mJ pulse energy, 4-ns pulse duration). The narrowband 202-nm light, which is tuned to the center of the two-photon transition, excites only molecules with a nearly zero velocity component along the direction of the laser beams; thus when the second laser is scanned, Doppler-free spectra of the highly excited states are obtained. The 202-nm light is polarized along the applied electric field, while the 400-nm light's polarization can be either along the field direction (π polarization) or perpendicular to it (σ polarization). Dissociation of the excited-state molecules into $H(1s)+H(n=2)$ atoms is detected by ionizing the excited atoms util-

izing a third dye laser operating at 656 nm (the wavelength of the Balmer-α transition), through one-photon resonant, two-photon ionization. The 656-nm pulse has a pulse energy of 5 mJ, a bandwidth of several wave numbers, and a duration of 5 ns. It nearly saturates the ionization of the excited atoms. This pulse is delayed by only several nanoseconds from the 400-nm pulse, so that we can detect the atoms in the shortlived (3-ns lifetime) $n=2$ hydrogen Stark states, which are produced by rapid dissociation in the electric field. The 656-nm light is intense enough that hydrogen atoms in all of the $n=2$ Stark substates are ionized with equal probability. The apparatus is sensitive to dissociation rates of $\sim 10^8$ s^{-1} or greater, and ionization rates of $\sim 10^7$ s^{-1} or greater.

The vacuum chamber is a six-way stainless steel cross, pumped by a magnetic bearing turbomolecular pump (Seiko model STP-300). The laser beams enter through two Suprasil windows and pass through a baffle system which reduces scattered light in the chamber, before crossing in the center of the chamber. At the chamber's center there are two parallel grids spaced 1 cm apart and 5 cm in diameter, across which the voltage is applied to produce the electric field and collect ions formed by the irradiation of the molecular hydrogen. A pulsed valve (NRC model BV-100) operating with a backing pressure of several torr of H_2 is the source of molecular hydrogen, producing a weakly collimated effusive beam which is directed between the field grids. The molecular hydrogen density at the laser crossing point is $\sim 10^{12}$ cm^{-3}. By measuring the threshold field for ionization of Kr, we estimate that the electric field in the region where the light beams and molecular beam cross is uniform to about 0.5%. The background pressure in the chamber while

the valve is operating at a 10-Hz repetition rate is $\sim 2 \times 10^{-6}$ Torr. Once the ions leave the region between the grids, they are accelerated by a second electric field into a field-free drift tube 20 cm in length, where they are mass analyzed by time-of-flight before they are detected by a dual microchannel plate detector. The ion signals are sent to a multichannel boxcar averager (PAR model 4402), whose output is read and stored by an LSI 11/73 computer as the 400-nm laser's wavelength is scanned. Typically, the computer averages 10 laser shots at each wavelength of the laser. Simultaneously, an optogalvanic spectrum of uranium lines from a hollow-cathode discharge lamp[47] is recorded, thereby allowing us to calibrate[48] the high-resolution spectra to an accuracy of about 0.1 cm^{-1}.

We have studied the energy region between the saddle point and the first zero-field ionization limit for electric field strengths ranging up to 3 kV/cm for both parahydrogen (excitation from the $[1s\sigma 2s\sigma + (2p\sigma)^2]\,^1\Sigma_g^+(v=0,\ J=0)$ level) and orthohydrogen (excitation from the $[1s\sigma 2s\sigma + (2p\sigma)^2]/\,^1\Sigma_g^+(v=0,\ J=1)$ level), with π- and σ-polarized light.

IV. RESULTS AND DISCUSSION

A. Low-resolution studies

Figure 2 shows the ionization and dissociation spectra for orthohydrogen in a weak electric field of 5 V/cm at low resolution using σ-polarized light, while Fig. 3 shows the spectra in the same energy region for the same polarization taken at a field strength of 3.0 kV/cm. Figure 4 shows the 3.0 kV/cm spectra for parahydrogen using σ-
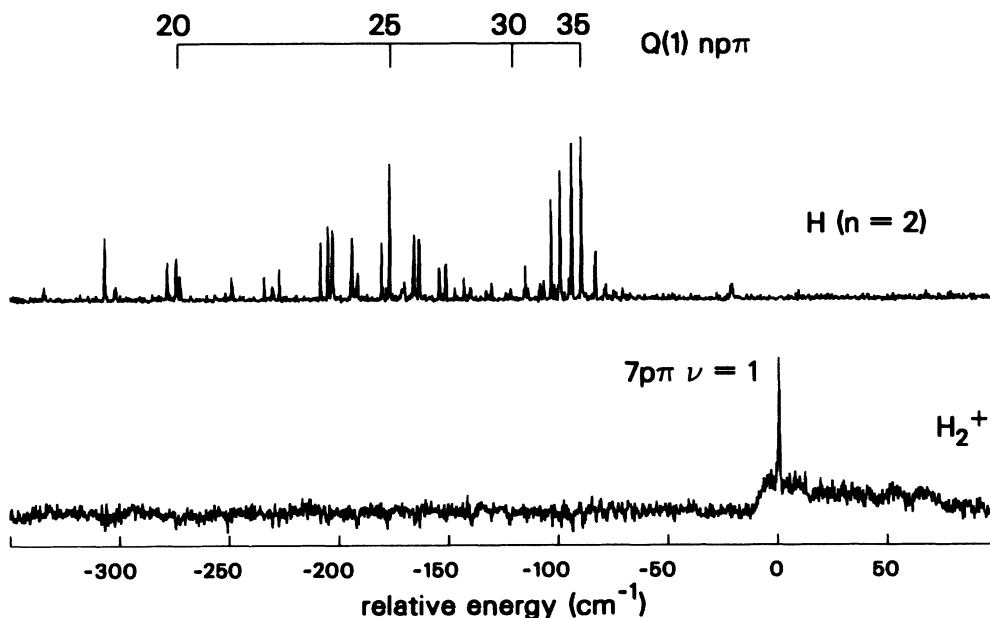

FIG. 2. Ionization and dissociation spectra of orthohydrogen taken with σ-polarized light in a weak static electric field of 5 V/cm. The top trace shows dissociation, while the bottom trace shows ionization. Q-branch ($\Delta J=0$) transitions to the $(1s\sigma np\pi)\,^1\Pi_u$ Rydberg levels which converge on the $v^+=0,\ N^+=1$ level of the molecular-ion core are noted with vertical lines. The narrow line in the ionization spectrum is due to the $(1s\sigma 7p\pi)\,^1\Pi_u(v^+=1)$ perturber level. The energy is measured with respect to the $v^+=0,\ N^+=1$ rotational level of the molecular-ion core $V_{\mathrm{ion}}+E_{\mathrm{ion}}(v^+=0,\ N^+=1)$. The vertical scale of each spectrum is arbitrary.
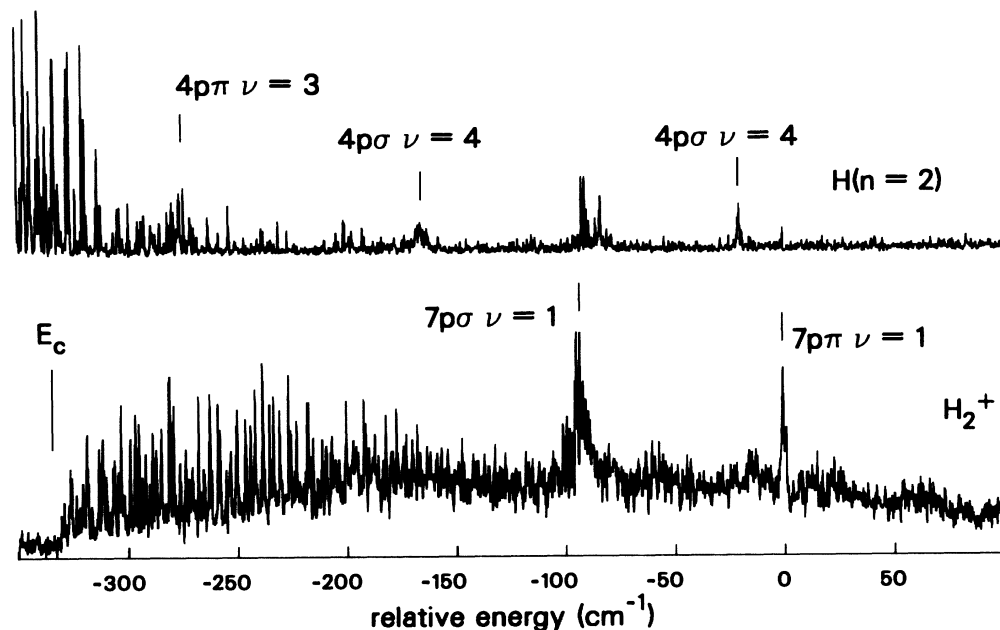
FIG. 3. Low-resolution ionization and dissociation spectra of orthohydrogen at an applied field strength of 3 kV/cm with σ-polarized light. The vertical lines denote the positions of perturber levels. The energy is measured with respect to the $v^+=0$, $N^+=1$ rotational level of the molecular-ion core $V_{ion}+E_{ion}(v^+=0,\ N^+=1)$. Again, the top trace shows dissociation, while the bottom trace shows ionization.

polarized light. In all of these figures, the top trace is the dissociation spectrum while the bottom trace is the ionization spectrum. The vertical scales of these figures are arbitrary, but we note that the dissociation and ionization spectra have roughly the same sensitivities. The zero of energy for the para spectrum is the zero-field $N^+=0$ ion-

ization limit, while the zero of energy for the ortho spectrum is the $N^+=1$ ionization limit. On the high-field spectra, the positions of known perturber levels[49] converging to excited vibrational levels of the core are denoted. The low field ionization spectrum shows no ionization other than background until the excitation energy is
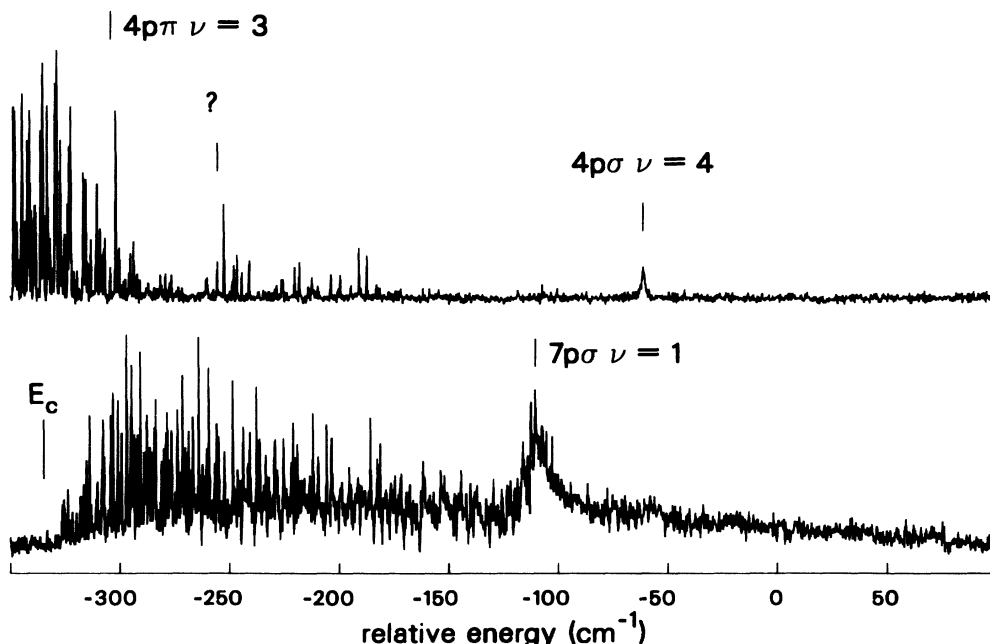

FIG. 4. Low-resolution ionization and dissociation spectra of parahydrogen at an applied field strength of 3 kV/cm with σ-polarized light. The vertical lines denote the positions of perturber levels. The energy is measured with respect to the adiabatic ionization potential of the molecule V_{ion}. The top trace shows dissociation, while the bottom trace shows ionization.

within a few wave numbers of the zero-field ionization potential; above this energy, direct photoionization occurs and autoionization structure is seen. The predissociation of the high np Rydberg levels is due to accidental near-degeneracies with predissociated Rydberg levels of low principle quantum number which are converging to excited rovibrational levels of the molecular-ion core.

The high-field spectra cover the energy range from below E_c for this field to above the zero-field ionization limit for $N^+=0$. Below E_c, the Stark states appear in the dissociative spectrum; since out detection time for dissociation is $\sim 10^{-9}$ s, these states are dissociating with rates on the order of 10^8 s^{-1} or greater. Because perturber levels are not nearby, we postulate that this dissociation is due to an electric-field induced couple between the highly excited Stark states and dissociative continua such as the $^1\Sigma_g$ continua. In this range of energy and electric-field strength, the highly excited Stark states are decaying almost exclusively by field-induced predissociation.

At the saddle-point energy the Stark states begin to appear in the ionization spectrum. In the energy region just above E_c, a number of Stark states appear in both decay channels. The competition of the decay channels in this energy region will be examined in detail later in this paper.

B. Forced autoionization of the $(1s\sigma 7p\sigma)\,^1\Sigma_u^+(v=1)$ levels

At energies well above E_c, the sharp structure in both ionization and dissociation dies out, except in special energy regions. In dissociation, a significant signal is seen in the region of perturbing states of low principle quantum number, whose positions are denoted in Figs. 3 and 4. We also note a small amount of field-induced predissociation of the ortho-H_2 $(1s\sigma 7p\pi)\,^1\Pi(v=1)$ autoionizing level. In ionization, a broad, asymmetric feature is seen in both the para and ortho spectra. In para-H_2 it peaks at ~ 109 cm^{-1} below the zero-field ionization limit, while in ortho-H_2 it peaks at ~ 93 cm^{-1} below this limit. This feature can be assigned as excitation of the $(1s\sigma 7p\sigma)\,^1\Sigma(v=1)$ level, which is undergoing forced autoionization in the electric field. There is also some enhancement of the dissociation signal at these energies. The shape of the forced autoionization resonance is similar to those of the higher members of the $(1s\sigma np\sigma)\,^1\Sigma(v=1)$ series which spontaneously autoionize, and its width of ~ 14 cm^{-1} is consistent with the n^{-3} scaling of autoionization widths in a series. These observations imply that levels from the $(1s\sigma 7p\sigma)\,^1\Sigma$ term couple to the lowered ionization continua through the same vibrational coupling which induces autoionization in the higher members of the series, and that any field-induced couplings which may be present are small in comparison to the vibrational coupling. We also note that the perturbing states which converge to ionic vibrational levels higher than $v=1$ are stable with respect to forced autoionization, indicating that the $\Delta v=-1$ propensity rule for vibrational autoionization is also followed in the presence of an electric field. This is to be expected, since the electric field should have a negligible effect on the vibrational levels of the ionic core.
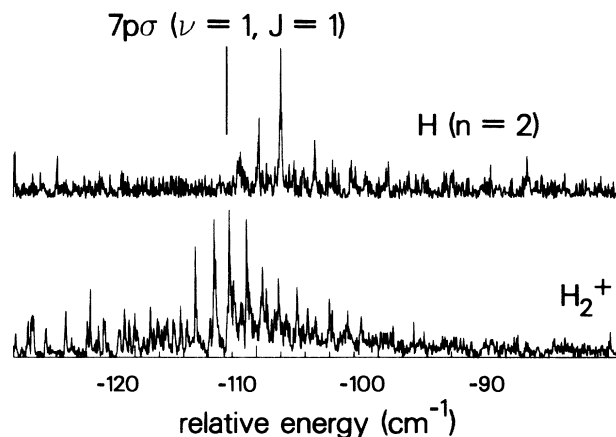

FIG. 5. High-resolution spectra of parahydrogen in the energy region near the $(1s\sigma 7p\sigma)\,^1\Sigma(v=1,\,J=1)$ level in an applied field of 750 V/cm. The energy is measured relative to the adiabatic ionization potential V_{ion}. The top trace shows dissociation, while the bottom trace shows ionization.

We have studied the forced autoionization of the $(1s\sigma 7p\sigma)\,^1\Sigma(v=1,\,J=1)$ resonance in parahydrogen at high resolution for several different magnitudes of the electric field. Some results, for σ-polarized light, are shown in Figs. 5–7. In these figures, the bottom trace is the ionization spectrum and the top trace is the dissociation spectrum. The vertical scales are arbitrary. Figure 5 shows the resonance at a field of 750-V/cm, Fig. 6 shows it at a field of 500 V/cm, and Fig. 7 shows it at a field of 300 V/cm. There are several remarkable features of these spectra. The forced autoionization resonance appears as an envelope of modulation of the intensities of the highly excited Stark states which are nearly degenerate with the $(1s\sigma 7p\sigma)\,^1\Sigma(v=1,\,J=1)$ level. This can be understood as being due to vibrational mixing between this level and the highly excited Stark states; since for the fields displayed here the only open ionization continuum is that belonging to the $N^+=0$ core state, the forced au-
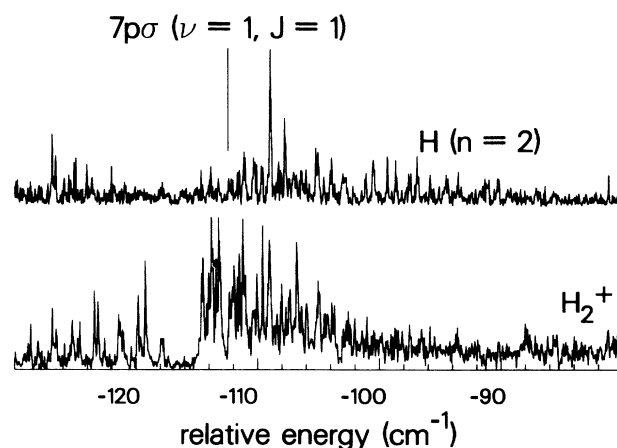

FIG. 6. High-resolution spectra in the same energy region as Fig. 5, but at a field strength of 500 V/cm.
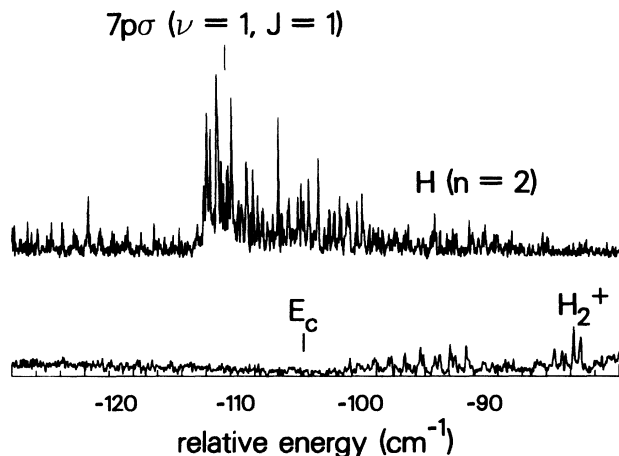
FIG. 7. High-resolution spectra in the same energy region as Figs. 5 and 6, but at a field strength of 300 V/cm.

toionization must occur through the structured continuum of these Stark states. Similar effects have recently been seen in atomic cesium.[50] At the two higher fields, the resonance is above E_c and ionization is classically allowed. In these cases, dissociation is only slightly enhanced, indicating that the ionization rates of the Stark components near the $(1s\sigma 7p\sigma)\,^1\Sigma(v=1,\ J=1)$ level are much higher than the dissociation rates. At the lowest field, shown in Fig. 7, ionization is classically forbidden and the resonance appears only in dissociation as a strong enhancement of the excitation and predissociation of the highly excited Stark states.

One very interesting feature of these spectra is the fact that the shape of the Fano profilelike envelope of modulations is a function of the electric field magnitude. The 500 V/cm spectrum in Fig. 6 shows a pronounced dip on its red wing which is absent from the 750-V/cm spectrum; presumably, this dip results from interference between the direct and indirect contributions to the photoexcitation, the process which gives rise to the asymmetry of the Fano profile. Thus, what we are seeing is a variation of the asymmetry parameter with the electric field. The asymmetry parameter q is given by the expression[51]

$$q = \frac{\langle \phi | T | i \rangle}{\pi \langle \psi_E | H | \Phi \rangle \langle \Psi | T | i \rangle},\qquad (8)$$

where $\langle \phi | T | i \rangle$ is the dipole matrix element between the initial state $|i\rangle$ and the mixed quasidiscrete final state $\langle \phi |$, the dipole matrix element between the initial state and the mixed structured Stark continuum is $\langle \Psi | T | i \rangle$, and $\langle \psi_E | H | \Phi \rangle$ is the coupling matrix element between the unmixed $(1s\sigma 7p\sigma)\,^1\Sigma(v=1,\ J=1)$ level $|\Phi\rangle$ and the unmixed Stark continuum $\langle \psi_E |$. Therefore, the variation in the asymmetry parameter could arise either from a field-induced component of the coupling or from a variation of the excitation dipole matrix elements of the Stark states. Since the 3-kV/cm spectra indicate that the coupling leading to forced autoionization is primarily vibrational in nature, the variation of the resonance shape must be due to the dependence of the excitation matrix element of the Stark states on the field magnitude at the energy of the $(1s\sigma 7p\sigma)\,^1\Sigma(v=1,\ J=1)$ level. Indeed, the background of Stark resonances appears to be significantly stronger in the 500-V/cm spectrum than in the 750-V/cm spectrum. This implies a smaller value of asymmetry parameter for the lower field, and a more asymmetric profile, as we observe.

Detailed analysis of the shapes of the envelopes would be difficult, since it would be complicated by the fact that there are actually a large number of series of Stark states involved, each of which may have different values of the matrix elements which determine the properties of the resonance shape. However, although the above arguments are highly simplified, we believe they contain the essence of this unexpected phenomenon.

C. High resolution studies near E_c

We now examine the high-resolution ionization and dissociation spectra of para-hydrogen in the region near E_c. We have taken spectra in this region for both σ and π polarization (we also have spectra of orthohydrogen, but those will not be presented here). Figure 8 shows the spectra for σ polarization at an electric field strength of 2.92 kV/cm, which results in excitation of pure $m_l=1$ states converging to the $N^+=0$ state of the ion. Figure 9 shows the spectra for π polarization, which excites pure $m_l=0$ states, at the same field strength. Again, the top traces show dissociation while the bottom traces show ionization. For both polarizations, we see a large number of very sharp resonances whose widths, in most cases, are predominantly instrumental. Specifically, some broadening results from the nonuniformity of the electric field in the sensitive region of the apparatus. The widths of the resonances are typically several tenths of a wave number. The sharpness of the resonances indicates that the Stark effect of these states is to some extent hydrogenic; that is, the shifts and broadening of the states by core-induced mixing are not severe. This is to be expected if the quantum defects of the various series being mixed by the field are all relatively small, as predicted by calculations for molecular hydrogen.[18] This observation implies that we may be able to identify the states using hydrogenic theory, except perhaps in the vicinity of avoided curve crossings. It is also interesting to note that in the σ-polarization ionization spectrum of Fig. 8, resonances do not appear until the energy is a few percent of E_c above E_c. This is to be expected if the excited states are pure $m_l=1$ states.[52]

We should note that the Stark spectra lack the strong localized perturbations which are seen in zero-field Rydberg spectra for parahydrogen, due to the interaction of the $N^+=0$ and $N^+=2$ series. In this energy region at a field strength of a few kV/cm, the $N^+=2$ states are Stark split almost to the point of mixing states of different principle quantum number, with the result that there is an $N^+=2$ Stark component every few wave numbers. Also, the interaction matrix element between two states of the different series depends on the square root of the product of the charge densities of the two states at the core. These charge densities are considerably smaller for the
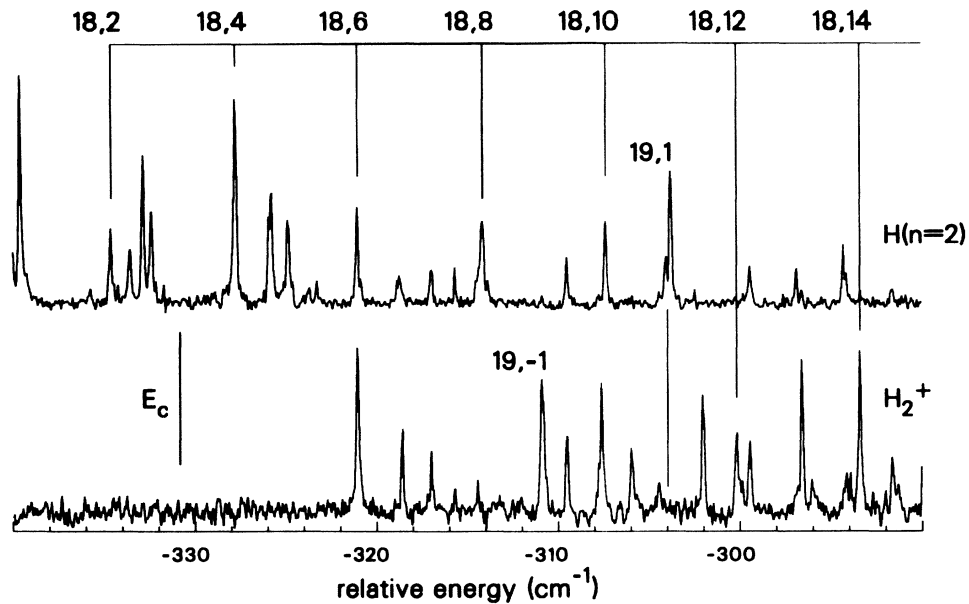
FIG. 8. High-resolution ionization and dissociation spectra of parahydrogen using σ-polarized light at a field strength of 2.92 kV/cm. The top trace shows dissociation, while the bottom trace shows ionization. The resonances are due to $m_1 = 1$ highly excited final states and are identified with the quantum numbers $n, n_1 - n_2$ by comparison to the results of hydrogenic theory given in Ref. 39. The energy is measured with respect to the adiabatic ionization potential V_{ion}.

FIG. 9. High-resolution ionization and dissociation spectra of parahydrogen using π-polarized light at a field strength of 2.92 kV/cm. The top trace shows dissociation, while the bottom trace shows ionization. The resonances are due to $m_1 = 0$ highly excited final states and are identified with the quantum numbers $n, n_1 - n_2$ by comparison to the results of hydrogenic theory given in Ref. 39. The energy is measured with respect to the adiabatic ionization potential V_{ion}.
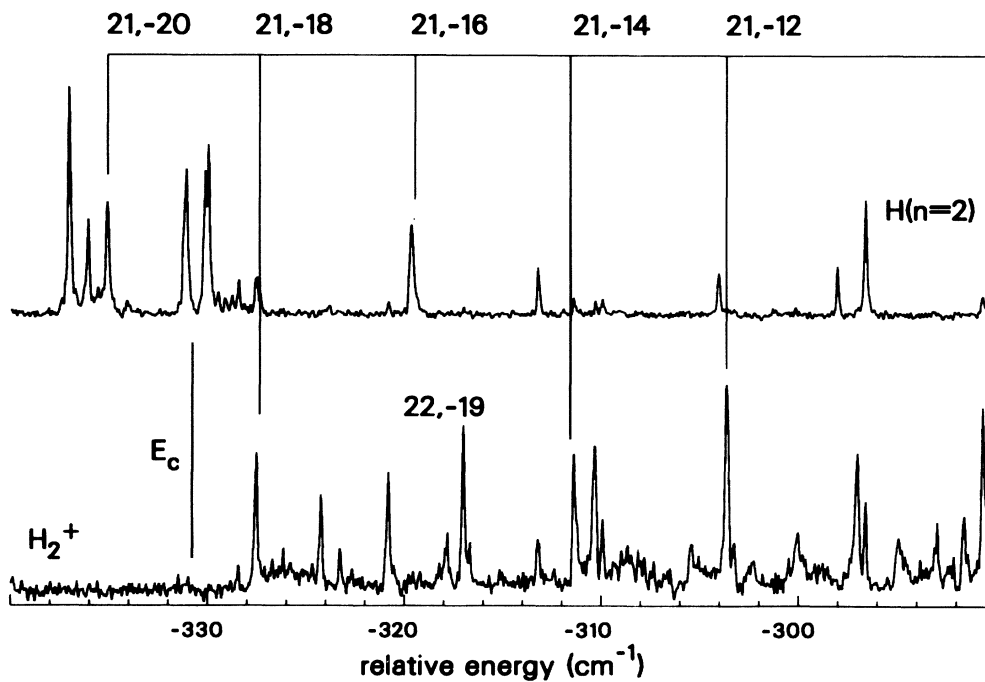
Stark states than for the field-free states; they are, in a sense, "spread out" among the Stark components. Thus the interaction between the Stark states of the two series is much weaker than in the field-free case. The net result of the spreading of the $N^+=2$ Stark components and the weakening of their interaction with the $N^+=0$ states is that their perturbations of the energies of the $N^+=0$ states are weak and diffuse, and can be neglected.

We have calculated the energies of the atomic hydrogenic Stark components in this energy region, in an attempt to identify the states responsible for the resonances in ionization and dissociation. Near E_c, fourth-order perturbation theory gives accurate energies for all but the most red shifted states but fails badly for the reddest states. Therefore, we have used the results of perturbation theory for the energies of most states, incorporating the geometric approximation for improved numerical accuracy;[53] for the significantly red shifted states, we use the results of numerical calculations.[39] The assigned quantum numbers of the identified states are shown in Figs. 8 and 9, given as $n, n_1 - n_2$. Table I gives the measured energies of the observed resonances in ionization and dissociation for $m_l = 1$ final states (excited by σ-polarized light), along with their assignments and the calculated energies of the assigned states. Table II presents the same information for $m_l = 0$ final states (excited by π-polarized light). [The calculated energies (see Footnote

b in Tables I and II) marked with a superscript "b" were calculated using the numerical theory of Ref. 39.] The agreement between the calculated and measured energies for the identified states is within a few tenths of a wave number. We do not see any lines corresponding to $N^+=2$ states. We also note that the states which are strongly excited do not follow the hydrogenic polarization dependence, although there is some preference for excitation of states of large $|n_1 - n_2|$ for π-polarized light and states of small $|n_1 - n_2|$ for σ-polarized light.

We will now discuss what these spectra tell us about the dynamics of the decay of the highly excited Stark states. If we examine Fig. 8 in which the final states should have $m_l = 1$ we see that some resonances appear in both ionization and dissociation, such as the $n = 18$, $n_1 - n_2 = 6$ resonance at -321.02 cm^{-1}, indicating that their ionization and dissociation rates are roughly equal. Other resonances such as the $n = 19$, $n_1 - n_2 = 1$ resonance at -303.76 cm^{-1} appear only in dissociation, while others such as the $n = 19$, $n_1 - n_2 = -1$ resonance at -310.84 cm^{-1} appear only in ionization. Thus the outcome of the competition between the decay channels of ionization and dissociation in this energy region can go in favor of either process.

In the case of isolated resonances, the dynamics of the excited state decay depends on the quantum numbers of

TABLE I. Measured and calculated energies of the highly excited $m_l = 1$, final Stark states at 2.92 kV/cm. Spectra are shown in Fig. 8.

| Measured energy[a] (cm^{-1}) | | Identification | Calculated energy |
Ionization	Dissociation	$n, n_1 - n_2$	(cm^{-1})
	-334.58	18,2	-334.51
	-333.53	17,15	-333.49
	-332.82	19,-7	-332.72
	-332.35	20,-14	-332.09
	-327.73	18,4	-327.73
	-325.80	19,-5	-325.75
-321.02	-321.01	18,6	-320.95
	-318.71		
-318.58		19,-3	-318.36^b
-316.95	-316.94	20-10	-317.10^b
-315.66	-315.65	21,-15	-315.52^b
-314.41			
	-314.13	18,8	-314.15
-310.84		19,-1	-311.06
-309.50	-309.48	20,-8	-309.83
-307.59		21,-13	-307.60^b
	-307.35	18,10	-307.34
-305.93			
	-303.76	19,1	-303.96
-301.99		20,-6	-302.06^b
-300.17		18,12	-300.52
-299.43	-299.41	21,-11	-299.67^b
	-296.85		
-296.56		19,3	-296.81
	-294.27	20,-4	-294.52^b
-293.39		18,14	-293.68

[a]Measured with respect to the adiabatic ionization potential V_{ion}.
[b]States calculated with the theory given in Ref. 39.

IONIZATION AND DISSOCIATION OF H_2 IN A STATIC . . .

TABLE II. Measured and calculated energies of the highly excited $m_l = 0$, final Stark states at 2.92 kV/cm. Spectra are shown in Fig. 9.

Measured energy[a] (cm^{-1})		Identification	Calculated energy
Ionization	Dissociation	$n, n_1 - n_2$	(cm^{-1})
	-337.02	$17, 14$	-336.71
	-336.05	$20, -15$	-335.81
	-335.08	$21, -20$	-335.25[b]
	-331.13	$18, 3$	-331.13
	-330.02	$17, 16$	-330.27
-327.54	-327.52	$21, -18$	-327.37[b]
-324.23		$18, 5$	-324.35
-320.82	-320.80	$20, -11$	-320.85[b]
	-319.63	$21, -16$	-319.48[b]
-317.83		$18, 7$	-317.55
-317.00		$22, -19$	-317.22[b]
-313.18	-313.19	$20, -9$	-313.36[b]
-311.37		$21, -14$	-311.57[b]
-310.31		$18, 9$	-310.75
	-304.02	$18, 11$	-303.94
-303.61		$21, -12$	-303.64[b]
	-298.00	$20, -5$	-298.30[b]
-297.00			
-296.56	-296.57		

[a]Measured with respect to the adiabatic ionization potential V_{ion}.
[b]States calculated with the theory given in Ref. 39.

the state in question. The predissociation rate of an isolated state is expected to vary roughly with the charge density of the excited state at the core (as n^{-3}), which is a rather slowly varying function of energy compared to the rapid increase of ionization rates as energies increase past E_c. It is for this reason that the resonances in the dissociation spectra die off rapidly above E_c while the ionization resonances persist to much higher energies (see Figs. 3 and 4). In the absence of state mixing, the states which appear as dissociation resonances should be those which have low ionization rates, i.e., those which have high values of n_1-n_2 and are below the top of their potential barrier.

The behavior described above does show up to a certain extent in the experimental spectra, but there are a number of resonances that do not behave this way. This is due to mixing of these states with other Stark states near avoided crossings. For example, in Fig. 8 the 18,6 resonance appears in both ionization and dissociation, while hydrogenic theory would predict a very low ionization rate for this state. It turns out that this state is very nearly degenerate with the red shifted 22,−20 state which has a very high ionization rate, and is therefore not visible as a discrete resonance in the spectrum. Mixing between these two states could give rise to the observable ionization of the 18,6 state. As we consider states of higher and higher energy, there are progressively more open ionization continue. At the high energy end of the spectra, the mixing between the Stark states which are stable in hydrogenic theory and the parabolic ionization continua is strong enough that ionization begins to dominate dissociation for all of the states.

Another interesting case is that of the 19,1 state at

-303.76 cm^{-1} which appears strongly in dissociation, while the neighboring states with $n = 19$ appear in ionization only. It seems likely that this behavior is due to this state's near degeneracy with the $(1s\sigma 4p\sigma)^1\Sigma(v=3, J=1)$ level, which has an energy of -304 cm^{-1}. This predissociated perturber will mix with the Stark state and enhance its dissociation rate. Thus we see that the dynamics of the Stark states is determined to a large degree by mixing with either other highly excited Stark states or perturbing states of low principle quantum number.

We now turn our attention to Fig. 9, which shows the excitation spectrum of $m_l = 0$ states. There are several notable differences between these spectra and the $m_l = 1$ spectra. First, there is a larger broad background in the ionization for the $m_l = 0$ spectrum than in the $m_l = 1$ spectrum, reflecting the higher excitation probability of red shifted, rapidly ionizing states in the $m_l = 0$ case. We also know that there are relatively fewer resonances appearing in dissociation for $m_l = 0$. This again suggests that the ns series quantum defect is somewhat larger than those of the np, nd, and other series, leading to stronger mixing of the parabolic channels and generally higher ionization rates. An interesting case of state mixing seems to be occurring at the position of the resonance labeled as 21,−16; which appears in dissociation but not in ionization. We would expect this red shifted state to be ionizing too rapidly for dissociation to be detectable if it were an isolated state; however, it is undergoing a curve crossing with the 23,−22 state and a near crossing with the 22,−19 state, both of which are ionizing too rapidly to be observable in the spectrum. The interactions of these states seem to lead to a stabilization of one of the mixed states, a phenomenon which has been studied in

complex atomic systems.[54] It is also possible that this line is actually due to an unidentified perturber state.

V. CONCLUSIONS

The Stark effect of molecular hydrogen in a strong electric field shows a variety of rich phenomena, some of which have parallels in atomic systems and some of which can only be studied in a molecular system. We have observed forced autoionization through the structured continuum of Stark states, electric-field-induced dissociation of Stark states, the ionization behavior of the Stark states of molecular hydrogen near E_c and the competition between the decay channels of ionization and dissociation. We find that the behavior of the highly excited states of H_2 is in many ways like that of atomic hydrogen, which is experimental evidence that the quantum defects of the various series are all rather small. However, the effects of mixing of the parabolic channels on the dynamics of the excited state decay are clearly present, in particular near curve crossings.

Further work on this topic should include the experimental generation of Stark maps of the ionization and dissociation spectra, absolute measurements of ionization rates and dissociation rates, and measurements of the quantum defects of the ns and nd Rydberg series of H_2. It would also be interesting to study the dissociation spectra of the Stark states with resolution of the atomic $n = 2$ Stark final states to gain additional information about the electric-field-induced dissociation process. These measurements will make a detailed comparison of experiment to the theory of the Stark effect in molecular hydrogen possible, as it develops.

*Present address: Department of Physics, Texas Tech University, Lubbock, Texas 79409-1051.

[1]E. Luc-Koenig and A. Bachelier, J. Phys. B **13**, 1743 (1980); **13**, 1769 (1980).

[2]D. A. Harmin, Phys. Rev. A **26**, 2656 (1982).

[3]Some of the numerous publications describing experimental studies of the strong-field Stark effect in complex atoms are R. R. Freeman and N. P. Economou, Phys. Rev. A **20**, 2356 (1979); S. Feneuile, S. Liberman, J. Pinard, and A. Taleb, Phys. Rev. Lett. **42**, 1404 (1979); T. S. Luk, L. DiMauro, T. Bergeman, and H. Metcalf, ibid. **47**, 2853 (1981); W. Sandner, K. A. Safinya, and T. F. Gallagher, Phys. Rev. A **23**, 2448 (1981); W. L. Glab, G. B. Hillard, and M. H. Nayfeh, ibid. **28**, 3682 (1983); C. Blondel, R. Champeau, and C. Delsart, J. Phys. B **18**, 2403 (1985).

[4]W. L. Glab and M. H. Nayfeh, Phys. Rev. A **31**, 530 (1985); W. L. Glab, K. Ng, D. Yao, and M. H. Nayfeh, ibid. **31**, 3677 (1985); H. Rottke and K. H. Welge, ibid. **33**, 301 (1986).

[5]D. A. Harmin, in *Atomic Excitation and Recombination in External Fields*, edited by M. H. Nayfeh and C. W. Clark (Gordon and Breach, New York, 1985), pp. 39–67.

[6]J. Chevaleyre, C. Bordas, M. Broyer, and P. Labastie, Phys. Rev. Lett. **557**, 3027 (1986).

[7]C. Bordas, P. F. Brevet, M. Broyer, J. Chevaleyre, P. Labastie, and J. P. Perrot, Phys. Rev. Lett. **60**, 917 (1988).

[8]G. R. Janik, O. C. Mullins, C. R. Mahon, and T. F. Gallagher, Phys. Rev. A **35**, 2345 (1987).

[9]E. Y. Xu, H. Helm, and R. Kachru, Phys. Rev. Lett. **59**, 1096 (1987).

[10]W. L. Glab and J. P. Hessler, Phys. Rev. A **35**, 2102 (1987).

[11]G. Herzberg, Phys. Rev. Lett. **23**, 1081 (1969).

[12]S. Takezawa, J. Chem. Phys. **52**, 2575 (1970).

[13]G. Herzberg and Ch. Jungen, J. Mol. Spectrosc. **41**, 425 (1972).

[14]Ch. Jungen and O. Atabek, J. Chem. Phys. **66**, 5584 (1977).

[15]Ch. Jungen, Phys. Rev. Lett. **53**, 2394 (1984).

[16]C. H. Greene and Ch. Jungen, Adv. At. Mol. Phys. **21**, 51 (1985).

[17]G. Herzberg, *Spectra of Diatomic Molecules* (Van Nostrand, New York, 1950), p. 217.

[18]Ch. Jungen (private communication).

[19]G. R. Cook and P. H. Metzger, J. Opt. Soc. Am. **54**, 968 (1964).

[20]K. D. Beyer and K. H. Welge, Z. Naturforsch. Teil A **19**, 19 (1964); **22**, 1161 (1967).

[21]F. J. Comes and H. O. Wellern, Z. Naturforsch. Teil A **23**, 881 (1968).

[22]J. E. Mentall and E. P. Gentieu, J. Chem. Phys. **52**, 5641 (1970).

[23]P. Borrell, P. M. Guyon, and M. Glass-Maujean, J. Chem. Phys. **66**, 818 (1977).

[24]M. Glass-Maujean, J. Breton, and P. M. Guyon, Chem. Phys. Lett. **63**, 591 (1979).

[25]P. J. Julienne, Chem. Phys. Lett. **8**, 27 (1971).

[26]F. Fiquet-Fayard and O. Gallais, Chem. Phys. Lett. **16**, 18 (1972).

[27]T. E. Sharp, At. Data **2**, 119 (1971).

[28]P. M. Guyon, J. Breton, and M. Glass-Maujean, Chem. Phys. Lett. **68**, 314 (1979).

[29]M. Glass-Maujean, Chem. Phys. Lett. **68**, 320 (1979).

[30]M. Glass-Maujean, J. Breton, B. Thiemblemont, and K. Ito, Phys. Rev. A **32**, 947 (1985).

[31]W. A. Chupka and J. Berkowitz, J. Chem. Phys. **51**, 4244 (1976).

[32]W. L. Glab and J. P. Hessler, Phys. Rev. Lett. **62**, 1472 (1989).

[33]H. A. Bethe and E. E. Salpeter, *Quantum Mechanics of One- and Two-Electron Atoms* (Plenum, New York, 1977), pp. 27–32.

[34]H. J. Silverstone, Phys. Rev. A **18**, 1853 (1978).

[35]P. M. Koch, Phys. Rev. Lett. **41**, 99 (1978).

[36]R. J. Damburg and V. V. Kolosov, J. Phys. B **9**, 3149 (1976).

[37]M. G. Littman, M. M. Kash, and D. Kleppner, Phys. Rev. Lett. **41**, 103 (1978).

[38]D. A. Harmin, Comments At. Mol. Phys. **15**, 281 (1985).

[39]G. B. Hillard and W. L. Glab, Physica **145C**, 229 (1987).

[40]J. W. Cooper, E. B. Saloman, B. E. Cole, and Shardanand,

Phys. Rev. A **28**, 1832 (1983).

[41]F. J. Comes and U. Wenning, Chem. Phys. Lett. **5**, 195 (1970).

[42]Ginette Jalbert, P. Labastie, P. F. Brevet, C. Bordas, and M. Broyer, Phys. Rev. A **40**, 784 (1989).

[43]K. Sakimoto, J. Phys. B **22**, 2727 (1989).

[44]W. L. Glab and J. P. Hessler, Appl. Opt. **26**, 3181 (1987).

[45]W. L. Glab, D. G. Ettinger, and J. P. Hessler (unpublished).

[46]W. L. Glab and J. P. Hessler, Appl. Opt. **27**, 5123 (1988).

[47]D. S. King, P. K. Schenck, K. C. Smyth, and J. C. Travis, Appl. Opt. **16**, 2617 (1977).

[48]B. A. Palmer, R. A. Keller, and R. Engleman, Jr., *An Atlas of Uranium Emission Intensities in a Hollow Cathode Discharge,*

Los Alamos Scientific Laboratory Informal Report No. LA-8251-MS, 1980 (unpublished).

[49]G. Herzberg and Ch. Jungen, J. Mol. Spectrosc. **41**, 425 (1972).

[50]C. Chardonnet, D. Delande, and J. C. Gay, Phys. Rev. A **39**, 1066 (1989).

[51]U. Fano, Phys. Rev. **124**, 1866 (1961).

[52]W. E. Cooke and T. F. Gallagher, Phys. Rev. A **17**, 1226 (1978).

[53]O. Goscinski and E. Brandas, Phys. Rev. **182**, 43 (1969).

[54]J.-Y. Liu, P. McNicholl, D. A. Harmin, J. Ivri, T. Bergeman, and H. J. Metcalf, Phys. Rev. Lett. **55**, 189 (1985).